Time decorrelation in isotropic magnetohydrodynamic turbulence



2011 EPL 96 55003

(http://iopscience.iop.org/0295-5075/96/5/55003)

A Letters Journal Exploring the Frontiers of Physics

December 2011

EPL, **96** (2011) 55003
doi: 10.1209/0295-5075/96/55003

www.epljournal.org

# Time decorrelation in isotropic magnetohydrodynamic turbulence

S. Servidio[1(a)], V. Carbone[1,2], P. Dmitruk[3] and W. H. Matthaeus[4]

[1] *Dipartimento di Fisica, Università della Calabria - I-87036 Cosenza, Italy, EU*
[2] *IPCF/CNR, Universitá della Calabria - I-87036 Cosenza, Italy, EU*
[3] *Departamento de Física, Facultad de Ciencias Exactas y Naturales, Universidad de Buenos Aires and IFIBA/CONICET - Buenos Aires 1428, Argentina*
[4] *Department of Physics and Astronomy, University of Delaware - Newark, DE 19716, USA*

received 1 July 2011; accepted in final form 19 October 2011
published online 24 November 2011

PACS 52.35.Ra – Plasma turbulence
PACS 52.30.Cv – Magnetohydrodynamics (including electron magnetohydrodynamics)
PACS 52.65.Kj – Magnetohydrodynamic and fluid equation

**Abstract** – Time decorrelation in isotropic incompressible magnetohydrodynamic (MHD) turbulence is studied using three-dimensional numerical simulation. Eulerian and wavenumber-dependent correlation functions are obtained. Scaling with wavenumber separates effects of nonlinear distortion and effects of random sweeping and Alfvénic wave propagation. Results show that the dominant effect is the combined influence of convective sweeping and Alfvénic propagation, both being nonlocal effects on small-scale fluctuations by large-scale fluctuations. This conclusion finds applications in space plasma observation, particle scattering, predictability, and turbulence theory.



Turbulent fluctuations are typically broad-band in spatial and temporal scales, while nonlinear couplings both generate and destroy correlations among fluctuations [1,2]. These interactions may be of several types, such as local-in-scale nonlinear distortion of eddies [1,3], or the transport or "sweeping" of small eddies by the large eddies [4–8]. Experimental studies in hydrodynamics have investigated time correlations through the Eulerian (single-point, two-time) correlation as well as the scale-dependent or "filtered" time correlation [9,10]. These measurements should not be confused with spatial correlations and spectra measured using the Taylor hypothesis [11]. Time decorrelation can be a controlling factor in spectral transfer, inertial range scaling, diffusion and other fundamental processes, and this role is especially evident in closures [2,12,13].

Here, we focus on the analogous problem of time decorrelation in magnetohydrodynamic (MHD) turbulence. Although less well studied, MHD temporal correlations are correspondingly important in space and astrophysical applications, entering into predictability, interpretation of spacecraft data, and charged-particle scattering. We will study time correlations in MHD by analysis of direct spectral-method numerical simulations.

Experimental [10,11,14] and simulation [15,16] studies in hydrodynamics, and related studies in space plasmas [17] and complex fluids [18], have characterized the Eulerian (single-point two-time) correlations, and when available, the more detailed scale-dependent (or "filtered") time correlation functions. The scale-dependent correlations are crucial in explaining the Eulerian frequency spectrum and the spectrum of accelerations [8]. Local arguments [1,3] based on nonlinear straining lead to a prediction[1] of the frequency spectrum of the Lagrangian velocity field $E_L(\omega) \sim \omega^{-2}$. On the other hand, random sweeping leads to a Eulerian frequency spectrum $E_E(\omega) \sim v^{2/3}\omega^{-5/3}$ [6,7]. The explicit appearance of the r.m.s. turbulence velocity $v$ indicates that sweeping is nonlocal. There has been some controversy in regarding hydrodynamic temporal decorrelation [7,8,19,20]. However, the prevailing conclusion [14–16] has been that sweeping dominates inertial range temporal decorrelation in hydrodynamics.

MHD turbulence has greater complexity than hydrodynamics since the magnetic field introduces effects such as wave-like couplings, even though turbulence does not readily lead to a simple frequency-wavenumber relationship [21]. Questions regarding the controlling time scales

(a) E-mail: servidio@bartol.udel.edu

[1] This in analogy to the inertial range spectrum $E_v(k) \sim k^{-5/3}$.

for temporal decorrelation in MHD remain unsolved [22]. Here we analyze time decorrelation in isotropic steady turbulence employing spectral-method numerical simulation of the three-dimensional MHD equations.

The incompressible MHD equations, in terms of the Elsässer variables $\boldsymbol{z}^{\pm} = \boldsymbol{v} \pm \boldsymbol{b}$, for velocity field $\boldsymbol{v}$ and magnetic field $\boldsymbol{b} = \boldsymbol{B}/\sqrt{4\pi\rho}$ (in Alfvén speed units, with constant density $\rho$), assume the form

$$\frac{\partial \boldsymbol{z}^{\pm}}{\partial t} = -\left(\boldsymbol{z}^{\mp} \cdot \boldsymbol{\nabla}\right)\boldsymbol{z}^{\pm} - \boldsymbol{\nabla} P + \nu \nabla^2 \boldsymbol{z}^{\pm}. \qquad (1)$$

All quantities are normalized to a characteristic length $L_0$ and a typical Alfvèn speed of the magnetic field fluctuations $v_0 = \sqrt{\langle b^2 \rangle / 4\pi\rho}$, where $\langle \bullet \rangle$ denotes a spatial average. The unit time is the Alfvèn crossing time $t_0 = L_0/v_0$. The total pressure $P$ enforces the incompressibility constraint $\boldsymbol{\nabla} \cdot \boldsymbol{z}^{\pm} = 0$, and $\nu^{-1}$ is the Reynolds number (here equal to the resistive Reynolds number).

Equations (1) are solved in a cubic periodic box of side $2\pi L_0$, using spectral-method algorithms. With $\nu = 0$ the scheme conserves energy (and cross-helicity) in the continuous time, spatially discrete equations. A second-order Runge-Kutta method is used for time integration. Aliasing is removed by a two-thirds rule truncation method. Results are reported here from a run with resolution of $256^3$ grid points that allow moderately long time integrations, needed for well-resolved frequency power spectra with a Reynolds number $\nu^{-1} = 400$. The numerical results reported here have been tested for accuracy in both space and time [23,24], by comparison of simulations with varying resolution (not shown here). The initial state consists of nonzero amplitudes for the $\boldsymbol{v}(\boldsymbol{k})$ and $\boldsymbol{b}(\boldsymbol{k})$, equipartitioned in the wavenumber shell $1 \leqslant k \leqslant 6$, with $k = |\boldsymbol{k}|$ (in units of $1/L_0$). Random phases have been chosen for both fields. The initial cross-helicity $H_c = \langle \boldsymbol{v} \cdot \boldsymbol{b} \rangle$ and magnetic helicity $H_m = \langle \boldsymbol{a} \cdot \boldsymbol{b} \rangle$ (brackets represent space averages and $\boldsymbol{b} = \nabla \times \boldsymbol{a}$) are small and remain negligible during the time evolution. To achieve a statistically steady state we consider driving which consist of maintaining constancy in time of Fourier modes in the band $0.9 < k < 3.5$. The total energy $E = 1/4 \langle |\boldsymbol{z}^+|^2 + |\boldsymbol{z}^-|^2 \rangle$ reaches a quasisteady level after few nonlinear times $\tau_{nl}$, while the global time integration is $100\tau_{nl}$. In analogy to hydrodynamics a simple estimate of the global nonlinear (or eddy turnover) time is $\tau_{nl} = \lambda/Z$, where $Z = \sqrt{2E}$ and $\lambda$ is an energy-containing length scale. Note that if $\lambda \sim L_0$ and $Z \sim v_0$ then $\tau_{nl} \sim t_0$.

After few nonlinear times, due to a statistical balance between driving and viscous dissipation, the system is in a fully turbulent steady state, with a resulting broadband power spectrum. Note that the associated dissipation (injection) rates are $\epsilon_{\pm} = \langle \nu |\boldsymbol{\nabla} \times \boldsymbol{z}^{\pm}|^2 \rangle$, and that, in this case, $\epsilon_+ \simeq \epsilon_-$ since $H_c \simeq 0$. In fig. 1 we report the Elsässer energy spectra $E^{\pm}(k) = 1/2 \sum |\boldsymbol{z}^{\pm}(\boldsymbol{k})|^2$ at time $t = 50$, where the sum is over directions of $\boldsymbol{k}$.

For MHD turbulence [13,25,26], in addition to the global nonlinear time $\tau_{nl}$, there are also time scales associated with scale-dependent (local) nonlinear effects, nonlocal sweeping, and wave propagation. The time scales can be defined for each of the Elsässer fields from analysis of eq. (1). Unlike hydrodynamic flows in which the velocity is self-advecting, the MHD case is more complex in that the Elsässer field $\boldsymbol{z}^-$ is responsible for the advection of $\boldsymbol{z}^+$ and vice versa. Equivalently, the magnetic and velocity field fluctuations mutually advect each other. From eq. (1) and simple scaling arguments, one can estimate different characteristic times. The local eddy turnover time can be defined as $\tau_{nl}^{\pm} \sim (k Z_k^{\mp})^{-1}$ where, for example, $Z_k^{\mp}$ is the amplitude of $\boldsymbol{z}^{\mp}$ due to fluctuations at scale $1/k$. This generalizes the eddy turnover time to include the influence of eddies of a certain size, while also taking the distinctive physics of MHD into account. In terms of energy spectra we estimate $\tau_{nl}^{\pm}(k) \sim [k\sqrt{kE^{\mp}(k)}]^{-1}$.

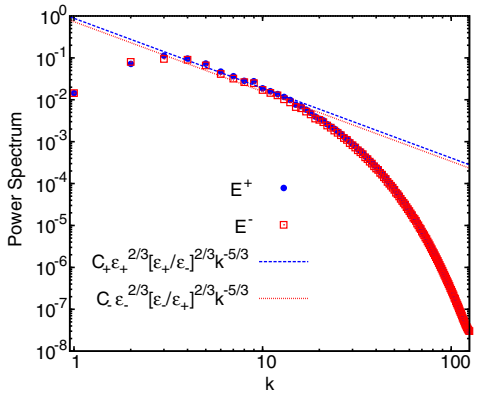


Fig. 1: (Color online) Elsässer energy spectral densities $E^+$ (blue bullets) and $E^-$ (red open squares) as a function of the wavenumber $k$. The dashed lines represent (see text) $E^{\pm} = C_{\pm}\epsilon_{\pm}^{2/3}[\epsilon_{\pm}/\epsilon_{\mp}]^{2/3}k^{-5/3}$, for $C_{\pm} = 2$, $\epsilon_+ = 0.26$ and $\epsilon_- = 0.24$.

For a Kolmogorov-style prediction (see [25]) of the MHD energy spectra, a key assumption is locality of spectral transfer. Thus, the development only involves the local nonlinear time scales $\tau_{nl}^{\pm}(k)$. Then (see [25,26]) one finds that $\epsilon_{\pm} = D_{\pm}(Z_k^{\pm})^2/\tau_{nl}^{\pm} = D_{\pm}k(Z_k^{\pm})^2 Z_k^{\mp} = D_{\pm}k^{5/2} \times E^{\pm}(k)\sqrt{E^{\mp}(k)}$, where $D_{\pm}$ are constants. From these two relations we conclude that the steady Kolmogorov-like high-Reynolds-number MHD energy spectra scale as $E^{\pm}(k) = C_{\pm}\epsilon_{\pm}^{2/3}[\epsilon_{\pm}/\epsilon_{\mp}]^{2/3}k^{-5/3}$. Thus, the nonlinear time scales in the inertial range can be approximately written as $\tau_{nl}^{\pm}(k) \sim [C_{\mp}^{1/2}\epsilon_{\mp}^{1/3}[\epsilon_{\mp}/\epsilon_{\pm}]^{1/3}k^{2/3}]^{-1}$. We note that the Elsässer energy spectra shown in fig. 1 admit a range of wavenumbers in which the spectral form roughly varies in accord with a $k^{-5/3}$ behavior.

The wavenumber spectra shown in fig. 1 are consistent with local scale-to-scale transfer dominated by nonlinearity and strain. However, the physics of time decorrelation is distinct and may still depend on other effects and therefore other available MHD time scales. One example is the advection (or sweeping) characteristic time at scale $1/k$, which may be expressed as $\tau_{sw}^{\pm}(k) \sim (k z_{rms}^{\mp})^{-1}$. In the latter, $z_{rms}^{\mp} = \langle |\boldsymbol{z}^{\mp}|^2 \rangle^{1/2}$ is a global quantity, typically

dominated by contributions from the large scales. Analogously, a characteristic Alfvèn time (averaged over direction, see [26]) can be defined as $\tau_A(k) \sim (k b_{rms})^{-1}$. The root-mean-square magnetic field $b_{rms}$ could in principle include contributions from both the fluctuations and a mean (uniform or very large scale) magnetic field[2]. For the simulation employed here, $b_{rms}$ is due only to fluctuations, which are assumed to have an isotropic distribution. It is worth noting that the sweeping and Alfvénic propagation time scales both vary as $\sim k^{-1}$. Finally, the viscous dissipation time is defined as $\tau_d(k) \sim (\nu k^2)^{-1}$. In the inertial region, for reasonably small values of $\nu$, both sweeping and eddy-turnover times are much smaller than the diffusive time. The Kolmogorov dissipation scale $\lambda_d$, defined as the scale at which $\tau_{nl} = \tau_d$, determines the termination of the inertial range. Generally speaking, in high Reynolds number turbulence, and for wavenumbers $k$ in the inertial range, we expect an ordering such that $\tau_d(k) > \tau_{nl}^{\pm}(k) > \tau_A(k) \simeq \tau_{sw}^{\pm}(k)$. Indeed, such ordering allows, among other things, the possibility of quasi-equilibrium properties within the inertial range [1].

Space-time structure for a given turbulent vector field, *e.g.*, the magnetic field $\boldsymbol{b}(\boldsymbol{x}, t)$ (this could also be $\boldsymbol{z}^{\pm}$, or $\boldsymbol{v}$), can be described by the two-point, two-time autocorrelation function $R(\boldsymbol{r}, \tau) = \langle \boldsymbol{b}(\boldsymbol{x}, t) \cdot \boldsymbol{b}(\boldsymbol{x} + \boldsymbol{r}, t + \tau) \rangle / \langle |\boldsymbol{b}|^2 \rangle$, computed at spatial and temporal lags $\boldsymbol{r}$ and $\tau$, respectively. The brackets indicate an ensemble average (and when appropriate, using the ergodic theorem, can be replaced by a spatial and/or temporal average). Fourier-transforming in $\boldsymbol{r}$ leads to the time-lagged spectral density which may be further factorized as $\hat{S}(\boldsymbol{k}, \tau) = S(\boldsymbol{k}) \Gamma(\boldsymbol{k}, \tau)$, where $\boldsymbol{k}$ is the wave vector. The function $\Gamma(\boldsymbol{k}, \tau)$, the scale-dependent (or "filtered") correlation function [9,10,15], represents the dynamical decorrelation effects. Describing the time decorrelation for each scale $k^{-1}$, the function $\Gamma$ is of central importance in turbulence closure models [1,2], and in charged-particle scattering in astrophysics [28]. (For scattering of high-energy cosmic rays the magnetostatic approximation $\Gamma = 1$ is adequate, but for lower energies "dynamical" turbulence becomes progressively more important.) The function $\Gamma$ also controls the Eulerian (single-point, two-time) correlation $R(0, \tau) = \int \mathrm{d}\omega E(\omega) \exp(i\omega\tau)$, where $E(\omega)$ is called the Eulerian frequency spectrum.

The functional form of the decorrelation function $\Gamma(k, \tau)$ can be introduced through either empirical or theoretical models. For example, in recent solar wind studies $E(\omega) \sim \exp(-t/\tau_c)$ was assumed to determine the correlation time $\tau_c$ from spacecraft observations [17]. However, a more physically motivated description may be obtained by building models for $\Gamma(\boldsymbol{k}, \tau)$ from the basic principles of nonlinear decay (or strain) [1], random sweeping [4,5], and Alfvénic propagation. (See, *e.g.*, [25,29].) One

[2]The unaveraged Alfvén time scale is $(\boldsymbol{k} \cdot \boldsymbol{B}_0)^{-1}$, where $\boldsymbol{B}_0$ is a mean magnetic field. This induces anisotropy [27] and the possibility of important additional time scale effects. Here we deal only with the isotropic case, with $\boldsymbol{B}_0 = 0$.

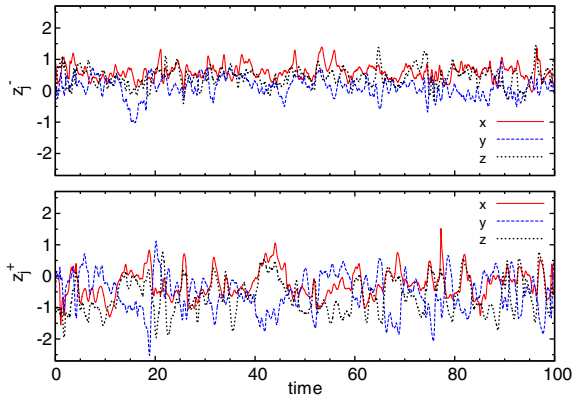


Fig. 2: (Color online) Time histories of $z_j^-(t)$ (top) and $z_j^+(t)$ (bottom) (with $j = x, y, z$) at a selected probe position.

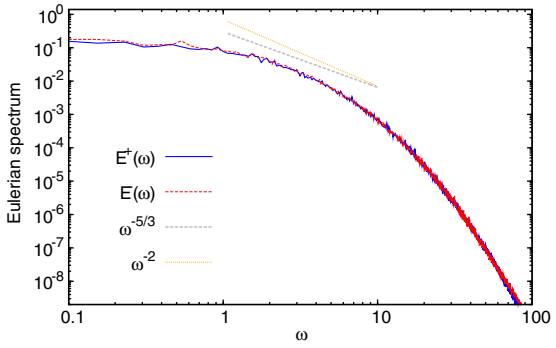


Fig. 3: (Color online) The Eulerian spectral densities $E^{\pm}(\omega)$ *vs.* $\omega$. Reference lines $\sim \omega^{-5/3}$ (dashed gray, corresponding to pure sweeping) and $\sim \omega^{-2}$ (dot-dashed orange, corresponding to pure local strain) are also shown. The computed Eulerian spectra do not readily distinguish these theories.

can then determine the Eulerian correlation as $R(0, \tau) = \int \mathrm{d}^3 k S(\boldsymbol{k}) \Gamma(\boldsymbol{k}, \tau)$.

In a first analysis of the present MHD simulations, we examine the Eulerian spectra and ask whether this will distinguish among the above physical processes. We proceed by obtaining the time series of the vectors $\boldsymbol{b}(t)$ and $\boldsymbol{v}(t)$ (and therefore $\boldsymbol{z}^{\pm}(t)$) at selected "probe" positions. Using a regular array of 64 points in a plane at the middle of the simulation box, we collect $\boldsymbol{z}_i^{\pm}(t)$ with a sampling time of $\delta t = 0.01$ (see [21]). Examples of these time series are shown in fig. 2. The Eulerian spectra (averaged over all probes) are shown in fig. 3. At high frequencies $1 < \omega < 10$, the behavior is intermediate to $\sim \omega^{-2}$ and $\sim \omega^{-5/3}$. Note that the frequency corresponding to the largest local nonlinear time is $\omega_0 = 2\pi/\tau_{nl(k=1)} \approx 1$. Apparently, it is difficult to distinguish between $\omega^{-2}$ and $\omega^{-5/3}$ in the Eulerian spectrum at this Reynolds number and resolution. The reason appears to be that the large eddies, for which neither sweeping nor inertial range straining are expected to be relevant, simply contribute too strongly near $\omega \simeq 1$, while the span of the inertial range contributions remains too narrow. This difficulty was long ago

seen in hydrodynamic turbulence studies wherein it was recognized that the scale- (wavenumber-) dependent time correlations will provide much more sensitive indicators of the dominant time decorrelation process [15,16]. We proceed to adopt the same strategy here.

From a theoretical perspective, the time correlations can be built up by specifying the time lag $\tau$ dependence of the scale-dependent time correlations $\Gamma(\boldsymbol{k},\tau)$ for all values of the wave vector $\boldsymbol{k}$. For isotropic turbulence the functional dependence is upon the wavenumber $k=|\boldsymbol{k}|$. It is reasonable to expect that these correlation functions assume a similarity form in terms of the underlying characteristic time scales, so that, assuming isotropy, $\Gamma(k,\tau)\to\Gamma(\tau/\tau_{nl}(k),\tau/\tau_{sw}(k),\tau/\tau_A(k)\ldots)$. In this view, the expectation is that $\Gamma=\Gamma[\eta(k)\tau]$ for some function of wavenumber $\eta$ that represents the composite effects of all underlying time scales at wavenumber $k$. In a work by Edwards [30], it has been argued that for many purposes an exponential form $\Gamma=\exp[\eta(k)\tau]$ adequately approximates the physics, provided that a correct $\eta(k)$ is identified. However, if one uses the $k$-dependent correlation time $\tau_C(k)$, then no assumption of the functional form needs to be made. Specifically, for the isotropic MHD Elsässer case the correlation times are

$$\tau_C^{\pm}(k)=\int_0^{\infty} R^{\pm}[\eta^{\pm}(k)\tau]\mathrm{d}\tau = C/\eta^{\pm}(k), \qquad (2)$$

where $C$ is a pure number. Consequently the functional dependence upon wavenumber of the correlation time is the same as that of $\Gamma(k,\tau)$.

In the event that one characteristic time scale exerts a dominant control over decorrelation in some range of wavenumbers, then in that range of $k$ the expectation is that $1/\eta$ is well approximated by that time scale. Therefore, for decorrelation that is dominated by local nonlinear strain effects, $\eta(k)\to 1/\tau_{nl}(k)$ and, from eq. (2), $\tau_c^{\pm}(k)\sim\tau_{nl}(k)\sim k^{-2/3}$. Alternatively, if the decorrelation is dominated by sweeping effects, as it happens in hydrodynamics at inertial range scales, then $\eta(k)\to 1/\tau_{sw}(k)$ and $\tau_c^{\pm}(k)\sim\tau_{sw}(k)\sim k^{-1}$. It is to be emphasized that the case of decorrelation governed by Alfvénic propagation [26] corresponds to $\eta(k)\sim\tau_A(k)\sim k^{-1}$.

We now proceed to analyze simulation data to estimate the variation with $k$ of the scale-dependent time correlation functions. With $\boldsymbol{z}^{\pm}(\boldsymbol{k},t)$ the Fourier amplitude of $\boldsymbol{z}^{\pm}$ at wave vector $\boldsymbol{k}$ at time $t$, we compute

$$Q^{\pm}(\boldsymbol{k},\tau)=\langle \boldsymbol{z}^{\pm}(\boldsymbol{k},t)\boldsymbol{z}^{\pm\star}(\boldsymbol{k},t+\tau)+\text{c.c.}\rangle_T, \qquad (3)$$

where $\tau$ represents the time increment, c.c. stands for complex conjugate, and now the brackets $\langle\ldots\rangle_T$ indicate that the average is computed over $\sim 81$ nonlinear times. From this expression we can define $R^{\pm}(k,\tau)$, which is an estimate of the isotropic scale-dependent correlation function $\Gamma(k,\tau)$, according to

$$\hat{R}^{\pm}(k,\tau)=\frac{Q^{\pm}(k,\tau)}{S^{\pm}(k)}, \qquad (4)$$

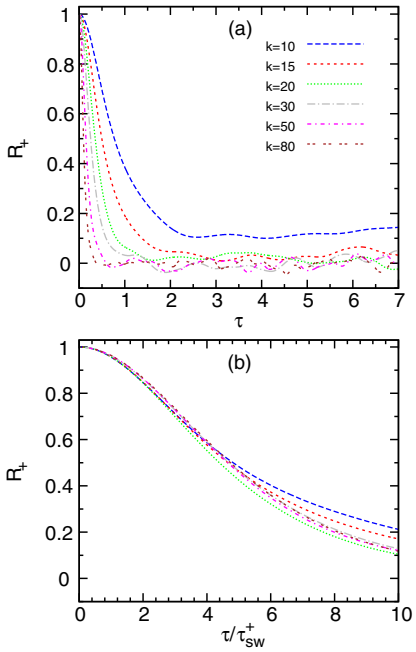


Fig. 4: (Color online) (a) Correlation functions $R^{+}(k,\tau)$ as a function of the lag time $\tau$, for different $k$-vectors. (b) Same correlation tensor with $\tau$ normalized to the sweeping characteristic time $\tau_{sw}$. The correlation function $R^{-}$ behaves in a similar way.

where $S^{\pm}(k)=Q^{\pm}(k,0)$ are the estimates of energy spectral density using the same time average procedure. The estimated correlation function $\hat{R}^{+}(k,\tau)$ is shown in fig. 4(a) for a selection of wavenumbers $k$. (The behavior of $\hat{R}^{-}$ is essentially the same.) It is evident that in all cases $\hat{R}^{\pm}(k,\tau)$ approaches zero with a rate that depends on the wave vector $k$. The higher $k$'s lose memory more rapidly than the lower $k$'s, as expected. A similar phenomenon can be observed in a low-order modeling of ideal MHD [31].

As indicated above, a key issue is the scaling of correlation times $\tau_C^{\pm}(k)$ with wavenumber $k$. Using the measured correlation functions and the definition in eq. (2), we fit the correlation times as $\tau_C^{\pm}(k)\sim k^{\alpha^{\pm}}$, and obtain an estimate for the exponents $\alpha^{\pm}$. In fig. 5 we report the computed $\tau_C^{\pm}(k)$ as a function of $k$. It is evident that the variation of the decorrelation times is closer to $k^{-1}$ than it is to $k^{-2/3}$. The best fit is given by $\alpha^{\pm}\simeq 1.10\pm 0.07$. In an attempt to collapse the data into a universal form, in fig. 4(b) we show as an example $\hat{R}^{+}(k,\tau)$ against $\tau$ normalized with respect to the sweeping time $\tau_{sw}^{+}$. The inertial– and near-dissipation–range wavenumbers demonstrate a good collapse with the sweeping normalization.

To distinguish in isotropic turbulence between sweeping and Alfvénic decorrelation, the latter being in effect "magnetic sweeping", simulations would need to be designed that maintain substantially different large scale flow speeds $u_{rms}$ and large scale Alfvén speeds $b_{rms}$. This would require the significant complication of

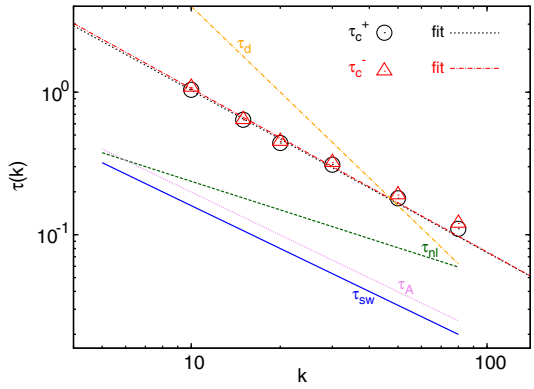


Fig. 5: (Color online) Correlation times $\tau_C^+(k)$ (black circles) and $\tau_C^-(k)$ (red triangles) as a function of $k$. Also shown are the best fits (dashed lines) $\tau_C^\pm(k) \sim k^{\alpha^\pm}$, obtained with $\alpha^\pm = 1.10 \pm 0.07$. For comparison, characteristic times are shown: $\tau_{nl}^\pm$ (green dashed), $\tau_A$ (pink dotted), $\tau_{sw}^\pm$ (blue full), and $\tau_d$ (orange dot-dashed).

either inverse cascade [13] or large scale "DC" magnetic field [27] and therefore lies beyond the scope of the present study.

In summary, we have investigated the degeneration of correlations in time for MHD turbulence in a model in which the flow is both incompressible and statistically isotropic. The study examined the temporal behavior of global, Eulerian correlation functions as well as scale-dependent or filtered correlations. The present results support the idea that random sweeping of the inertial range fluctuations by the large eddies, together with the Alfvèn propagation effect, are the principal phenomena producing decorrelation of the inertial range fluctuations. This conclusion is complementary to earlier observations and computations in hydrodynamics, which have confirmed that sweeping is the dominant process in the space-time dynamics of turbulence [15,16].

The present study confirms that there is a clear advantage in employing the scale-dependent analysis to identify dominant inertial range time scales. The Eulerian frequency spectrum $E(\omega)$ is less sensitive as can be seen by examining its structure,

$$E(\omega) = \left(\frac{1}{2\pi}\right)^4 \int \mathrm{d}^3k\, S(\boldsymbol{k}) \left[\int \mathrm{d}\tau\, e^{-i\omega\tau} \Gamma(\boldsymbol{k},\tau)\right], \quad (5)$$

which involves contributions from all wavenumbers. Even if sweeping dominates in the inertial range, this may not be evident in the Eulerian spectrum, which can always be expected to include a substantial contribution from the larger energy-containing scales. The lowest $k$ modes, for which neither nonlinear distortion nor sweeping/Alfvénic decorrelation is accurate, will have a time-dependence of distinct origin. In fact, it is known that for the largest scale ($k = 1$ mode) the frequency spectrum shows a $1/\omega$ behavior indicating very long-time fluctuations and the lacking of a single correlation time [32]. In summary, the weighting by the spectrum $S(\boldsymbol{k})$ in eq. (5) essentially guarantees that the decorrelation rates associated with the energetically dominant scales will substantially influence the functional form of the Eulerian spectrum.

A final remark on the role of anisotropy is relevant at this point. Throughout this paper we have assumed global statistical isotropy, and that the residual anisotropy in the inertial range is small. This stands in contrast to the well-known correlation and spectral anisotropy that occurs due to a large scale magnetic field [27,33–35], as well as the *local* anisotropy induced in subregions of isotropic turbulence [36–38]. Although the Eulerian spectrum is a one-point statistic, it is clear from eq. (5) that anisotropic effects can enter through $\Gamma$, while local anisotropic effects might influence locally defined versions of eq. (5). Examination of such issues would require substantial extension to the present approach in the form of conditional or local averaging procedures; such study is deferred to future works.

The present understanding of MHD time correlation is expected to have different applications, for example in charged-particle scattering theory, in the interpretation of interplanetary and magnetospheric spacecraft data, and in the predictability of interplanetary disturbances in the context of Space Weather.

* * *

This research has been supported in part by grants from FP7-PEOPLE-2010-IRSES, Proposal 269297 "TURBOPLASMAS", and by US NSF (Solar Terrestrial Program, AGS-1063439 and SHINE, ATM-0752135), NASA (Heliophysics Theory Program, NNX08AI47G, Heliophysics Guest Investigator Program NNX09AG31G) and Argentina UBACYT 20020090200602, PICT 2007-00856 and PIP 11220090100825.

REFERENCES

[1] Monin A. S. and Yaglom M., *Statistical Fluid Mechanics: Mechanics of Turbulence* (Dover, New York) 2007.
[2] McComb W. D., *The Physics of Fluid Turbulence* (Oxford University Press, New York) 1990.
[3] Kolmogorov A. N., *C. R. Acad. Sci. URSS*, **36** (1941) 301.
[4] Kraichnan R. H., *J. Fluid Mech.*, **5** (1959) 497.
[5] Kraichnan R. H., *Phys. Fluids*, **7** (1964) 1723.
[6] Tennekes H., *J. Fluid Mech.*, **67** (1975) 561.
[7] Chen S. and Kraichnan R. H., *Phys. Fluids A*, **1** (1989) 2019.
[8] Nelkin M. and Tabor M., *Phys. Fluids A*, **2** (1990) 81.
[9] Heisenberg W., *Z. Phys. A*, **124** (1948) 628 (translated into English in *NACA TM*, 1431 (1958)).
[10] Comte-Bellot G. and Corrsin S., *J. Fluid Mech.*, **48** (1971) 273.
[11] Van Atta C. W. and Wyngaard J. C., *J. Fluid Mech.*, **72** (1975) 673.
[12] Orszag S. A., *J. Fluid Mech.*, **41** (1970) 363.

[13] Pouquet A., Frisch U. and Léorat J., *J. Fluid Mech.*, **77** (1976) 321.
[14] Zhou Y., Praskovsky A. and Vahala G., *Phys. Lett. A*, **178** (1993) 138.
[15] Orszag S. A. and Patterson G. S., *Phys. Rev. Lett.*, **28** (1972) 76.
[16] Sanada T. and Shanmugasundaram V., *Phys. Fluids A*, **4** (1992) 1245.
[17] Matthaeus W. H., Dasso S., Weygand J. M., Kivelson M. G. and Osman K. T., *Astrophys. J.*, **721** (2010) L10.
[18] Carbone F., Sorriso-Valvo L., Versace C., Strangi G. and Bartolino R., *Phys. Rev. Lett.*, **106** (2011) 114502.
[19] Yakhot V., Orszag S. A. and She Z.-S., *Phys. Fluids A*, **1** (1989) 184.
[20] McComb W. D., Shanmugasundaram V. and Hutchinson P., *J. Fluid Mech.*, **208** (1989) 91.
[21] Dmitruk P. and Matthaeus W. H., *Phys. Plasmas*, **16** (2009) 062304.
[22] Busse A., Müller W.-C. and Gogoberidze G., *Phys. Rev. Lett.*, **105** (2010) 235005.
[23] Wan M., Oughton S., Servidio S. and Matthaeus W. H., *Phys. Plasmas*, **17** (2010) 082308.
[24] Yeung P. K., Pope S. B. and Sawford B. L., *J. Turbul.*, **7** (2006) 58.
[25] Zhou Y., Matthaeus W. H. and Dmitruk P., *Rev. Mod. Phys.*, **76** (2004) 1015.
[26] Kraichnan R., *Phys. Fluids*, **8** (1965) 1385.
[27] Shebalin J. V., Matthaeus W. H. and Montgomery D., *J. Plasma Phys.*, **29** (1983) 525.
[28] Bieber J. W. *et al.*, *Astrophys. J.*, **420** (1994) 294; Matthaeus W. H. and Bieber J., in *Solar Wind 9*, edited by Habbal S. R., Esser R., Hollweg J. V. and Isenberg P. A., *AIP Conf. Proc.*, **471** (1999) 515.
[29] Shalchi A., Bieber J. W., Matthaeus W. H. and Schlickeiser R., *Astrophys. J.*, **642** (2006) 230.
[30] Edwards S. F., *J. Fluid Mech.*, **18** (1964) 239.
[31] Servidio S., Matthaeus W. H. and Carbone V., *Phys. Rev. E*, **78** (2008) 046302.
[32] Dmitruk P. and Matthaeus W. H., *Phys. Rev. E*, **76** (2007) 036305; Dmitruk P., Mininni P. D., Pouquet A., Servidio S. and Matthaeus W. H., *Phys. Rev. E*, **83** (2011) 066318.
[33] Oughton S., Priest E. R. and Matthaeus W. H., *J. Fluid Mech.*, **280** (1994) 95.
[34] Carbone V. and Veltri P., *Geophys. Astrophys. Fluid Dyn.*, **52** (1990) 153.
[35] Carbone V., Malara F. and Veltri P., *J. Geophys. Res.*, **100** (1995) 1763.
[36] Cho J. and Vishniac E. T., *Astrophys. J.*, **539** (2000) 273.
[37] Milano L. J., Matthaeus W. H., Dmitruk P. and Montgomery D. C., *Phys. Plasmas*, **8** (2001) 2673.
[38] Sorriso-Valvo L., Carbone V., Bruno R. and Veltri P., *Europhys. Lett.*, **75** (2006) 832.